Stem Cell Reports
Article
OPEN ACCESS

Cell Division Mode Change Mediates the Regulation of Cerebellar Granule Neurogenesis Controlled by the Sonic Hedgehog Signaling

Rong Yang,[1] Minglei Wang,[1] Jia Wang,[1] Xingxu Huang,[2] Ru Yang,[1,*] and Wei-Qiang Gao[1,3,*]
[1]State Key Laboratory of Oncogenes and Related Genes, Renji-MedX Stem Cell Research Center, Ren Ji Hospital, School of Biomedical Engineering, Shanghai Jiao Tong University, Shanghai 200030, China
[2]School of Life Science and Technology, ShanghaiTech University, Shanghai 200031, China
[3]Collaborative Innovation Center of Systems Biomedicine, Shanghai 200240, China
*Correspondence: yangru@yahoo.com (R.Y.), gao.weiqiang@sjtu.edu.cn (W.-Q.G.)
http://dx.doi.org/10.1016/j.stemcr.2015.09.019

SUMMARY

Symmetric and asymmetric divisions are important for self-renewal and differentiation of stem cells during neurogenesis. Although cerebellar granule neurogenesis is controlled by sonic hedgehog (SHH) signaling, whether and how this process is mediated by regulation of cell division modes have not been determined. Here, using time-lapse imaging and cell culture from neuronal progenitor-specific and differentiated neuron-specific reporter mouse lines (*Math1-GFP* and *Dcx-DsRed*) and *Patched*$^{+/-}$ mice in which SHH signaling is activated, we find evidence for the existence of symmetric and asymmetric divisions that are closely associated with progenitor proliferation and differentiation. While activation of the SHH pathway enhances symmetric progenitor cell divisions, blockade of the SHH pathway reverses the cell division mode change in *Math1-GFP;Dcx-DsRed;Patched*$^{+/-}$ mice by promoting asymmetric divisions or terminal neuronal symmetric divisions. Thus, cell division mode change mediates the regulation of cerebellar granule neurogenesis controlled by SHH signaling.

INTRODUCTION

Cell division mode studies have been mainly carried out in the embryogenesis of the invertebrates such as *Drosophila* and *C. elegans* where self-renewal and cell fate specification of stem cells are accurately controlled (Bertrand and Hobert, 2009; Knoblich, 2008; Li et al., 2013b). Cell division modes include both symmetric and asymmetric divisions. The former can be further categorized as non-terminal symmetric divisions and terminal symmetric divisions. By non-terminal symmetric divisions, progenitor cells can generate two progenitor cells, expanding the progenitor pool. By terminal symmetric divisions, a progenitor cell produces two differentiated neurons, thus gradually depleting the progenitor pool. However, by asymmetric progenitor divisions, a progenitor generates one progenitor cell and one differentiated neuron, maintaining the progenitor pool and producing the differentiated progeny. Recent studies have shown that these cell division modes are also observed in the developing mammalian neocortex (Gao et al., 2014; Noctor et al., 2004; Wang et al., 2009; Zhong, 2008; Zhong and Chia, 2008; Zhou et al., 2007). However, whether a similar mechanism occurs elsewhere in the mammalian CNS, such as the cerebellum, is poorly studied.

Cerebellar development exhibits a lot of unique features that are different from cerebral neurogenesis. While most cerebral neurons are generated from the ventricle zone residing in the deep layer of cortex, cerebellar granule cells are produced in the outside of the cerebellum (Hatten and Heintz, 1995). In addition, unlike most cerebral neuronal stem cells, cerebellar granule neuronal progenitors (GNPs) are highly proliferative cells that remain active in mitosis in the external granule layer (EGL) even after birth. During the first 2–3 postnatal weeks, GNPs differentiate, exit the cell cycle, and migrate inward to form the internal granule layer, with EGL disappearing in parallel gradually. The spatiotemporal steps of proliferation and differentiation of GNPs have been described in our previous work (Gao et al., 1991; Gao and Hatten, 1993). Recent studies have demonstrated that sonic hedgehog (SHH) secreted by Purkinje cells can regulate the proliferation of GNPs (Wechsler-Reya and Scott, 1999). When treated with recombinant SHH, GNPs can be induced to undergo a long-lasting proliferation, preventing them from differentiation. However, whether such effects by SHH are mediated by changes of symmetric and asymmetric divisions of GNPs has not been studied.

In this study, we performed cell division mode analyses using various GNP-specific and differentiated granule neuron (GN)-specific reporter mice and carried out fluorescence confocal or multi-photon microscopy and time-lapse image acquisition experiments in cell cultures, as well as in freshly dissected whole-mount cerebella (ex vivo). We found evidence for the existence of non-terminal symmetric divisions, terminal symmetric divisions, and asymmetric divisions by GNPs. More importantly, activation of the SHH pathway in *Patched*$^{+/-}$ mutant mice increased proliferation and the number of GNPs by enhancing non-terminal symmetric cell divisions. On the contrary,

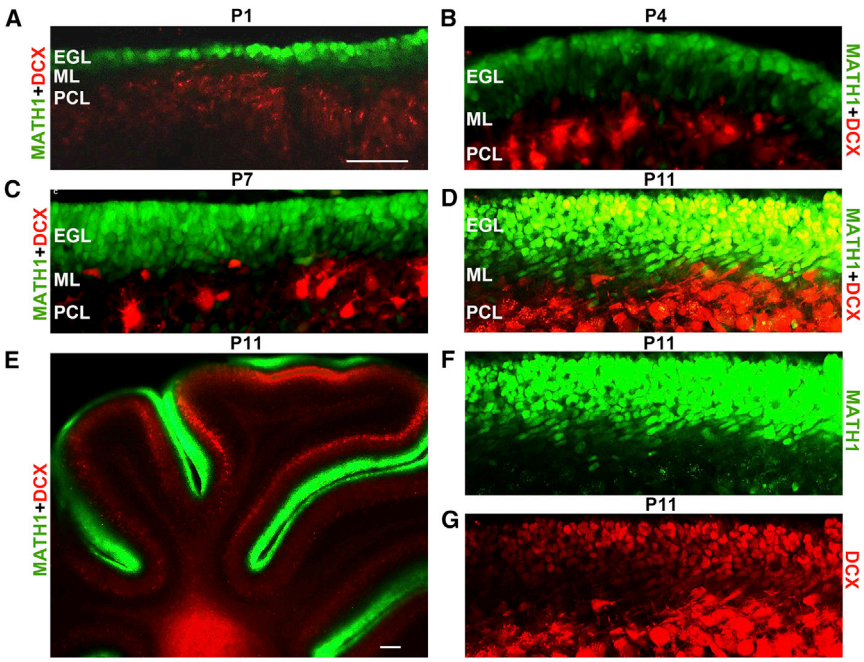

Figure 1. Characterization of *Math1-GFP;Dcx-DsRed* Mice

Math1-GFP;Dcx-DsRed mice strains were developed by crossing transgenic *Math1-GFP* and transgenic *Dcx-DsRed* mice. Cerebellar slices shown in P1 (postnatal day 1) (A), P4 (B), P7 (C), and P11 (D–G) indicate that progenitor cells are present in EGL at P1, increase in numbers at P4 and P7, and reach the number peak at P11, which is consistent with previous reports. MATH1 refers to cerebellar progenitor cells, and DCX is a biomarker of differentiated cells. MATH1 and DCX co-expressing cells represent a cell population at an intermediate stage of differentiation, undergoing a switch from MATH1-expressing cells to DCX-expressing cells, which are termed intermediate cells. See also Figure S1.

Scale bars, 60 μm for (A–D), (F), and (G) and 200 μm for (E).

administration of a small molecule inhibitor of the SHH pathway elicited the opposite effect, shifting the cell divisions to more asymmetric divisions. Thus, cell division mode changes mediate the regulation of GN neurogenesis governed by SHH signaling.

RESULTS

Math1-GFP;Dcx-DsRed Mice Are a Useful Model to Study Neurogenesis in the Cerebellum

To investigate cell division modes, cell fate specification, and neuronal differentiation in the cerebellum, we first introduced *Math1-GFP* and *Dcx-DsRed* mice from the Jackson Laboratory or Novartis, and then generated *Math1-GFP;Dcx-DsRed* mice by intercrossing the two lines. While MATH1 is a marker for cerebellar granule progenitors (Ben-Arie et al., 1997; Lumpkin et al., 2003), DCX (doublecortin) is specifically expressed by the early differentiated cerebellar GNs that just come out of the terminal mitosis (Francis et al., 1999; Gleeson et al., 1999; Wang et al., 2007). With the *Math1-GFP;Dcx-DsRed* mice, both progenitors and differentiated GNs could easily been observed in vivo or in dissociated cell cultures. An example of the well-labeled cells at postnatal day 11 (P11) is shown in Figure 1. While green fluorescent staining represented progenitor cells, red fluorescent labeling showed differentiated GNs. Yellow fluorescent staining displayed cells that were at an intermediate stage before acquisition of the differentiated neuronal fate. Therefore, the *Math1-GFP;Dcx-DsRed* mouse line provides an informative system for studying temporal GN neurogenesis, including self-renewal, cell fate specification, and neuronal differentiation.

GNPs Switch Gradually from MATH1-Expressing to DCX-Expressing Cells

To directly visualize the GNPs and differentiated GNs, we performed multi-photon microscopy of sagittal cerebellar sections prepared from *Math1-GFP;Dcx-DsRed* double reporter mice at various developmental stages ranging from P1 to P11. We observed a stepwise pattern of cerebellar neurogenesis during development. As shown in Figure 1, MATH1-positive cells were initially detectable in the EGL at P1 (Figure 1A), increased in numbers at P4 and P7 (Figures 1B and 1C), and reached a peak at P11 (Figures 1D–1G). In contrast, DCX-positive cells did not appear in the EGL until P7 and P11. In particular, many yellow fluorescent cells, a cell population co-expressing MATH1 and DCX, emerged at P11 (Figures 1D and 1E). This population appeared to represent the cells undergoing a switch from MATH1-expressing cells to DCX-expressing cells. We termed the yellow subpopulation intermediate cells; these have not been described previously.

Morphologically, we found that MATH1-GFP-positive GNPs looked like epithelioid cells based on the green and red fluorescence of *Math1-GFP;Dcx-DsRed* mice in vivo (Figure S1A). In contrast, DCX-DSRED-positive GNs appeared more like polyhedral cells with processes (Ryder and Cepko, 1994) (Figure S1B), and MATH1-GFP/DCX-DSRED double-positive intermediate cells were at the stage of changing from epithelioid cells to polyhedral cells (Figures

S1A and S1B), which quickly extended out processes (Figure S1B and Movie S1). We also found that GNPs were not stained by an antibody against neuron-glial antigen 2, which labels polydendrocytes (Nishiyama et al., 2009) or polyhedral cells, indicating that GNPs are not polyhedral cells (Figure S1C).

Cerebellar GNPs Display Both Symmetric and Asymmetric Divisions In Vitro and Ex Vivo

Given that the GNs originate from MATH1-positive GNPs in EGL (Machold and Fishell, 2005), we carried out primary cultures as previously described (Gao et al., 1991; Gao and Hatten, 1993) using *Math1-GFP;Dcx-DsRed* mice and recorded the cell division process using time-lapse imaging technology. The time-lapse imaging was performed for 72 hr with a fixed 6-min interval after the initial cell plating.

We adopted a practical definition to describe the different modes of cell divisions. If the fluorescence of the daughter cells is the same, the cell divisions are symmetric; if the fluorescence of the daughter cells is different, the cell divisions are asymmetric. In this way, we found that all MATH1-positive GNPs underwent symmetric divisions at P4 (Figure 2A), in which a progenitor cell was divided to generate two progenitor cells. Comparing to cell division modes in P4, we found that not all GNPs displayed symmetric divisions at P10. Among the total cell divisions identified in the time-lapse recording, 89.23% were symmetric divisions (Figures 2A and 2D and Movie S2) and 10.77% were asymmetric divisions (Figure 2B) at P10. Unlike the common asymmetric cell division that gives rise to one progenitor daughter cell and one differentiated daughter cell, the asymmetric divisions that we observed at P10 displayed a MATH1-positive progenitor that generated a MATH1-positive daughter cell and a MATH1/DCX co-expressing daughter cell (Figure 2B and Movie S3). This intermediate cell during the asymmetric division of GNPs in the developing cerebellum is the same as we described earlier in the sagittal cerebellar sections prepared from *Math1-GFP;Dcx-DsRed* mice at P11 (Figure 1D). To further characterize the intermediate cells, we traced these yellow cells and observed that they gradually turned from MATH1/DCX co-expression (yellow) cells to DCX-positive (red) cells (Figure 2C). Of the 79 MATH1-GFP and DCX-DSRED double-positive (yellow) progenitor cells that were traced in time-lapse recording, all yellow cells were observed to turn into red cells gradually and never underwent cell divisions (Figure 2C). Thus, the double-positive (yellow) cells represent newborn neurons, rather than transient amplifying cells or intermediate neural progenitor or precursor cells reported in the forebrain (Noctor et al., 2004). These in vitro time-lapse recording data also indicated that GNPs could undergo both symmetric and asymmetric divisions and that asymmetric progenitor divisions could be presented by a progenitor cell and an intermediate cell in the developing cerebellum.

To further confirm that symmetric and asymmetric cell divisions of GNPs exist in the developing cerebellum in vivo, we examined the progenitor divisions and the fates of their offspring cells in freshly dissected whole-mount cerebella from *Math1-GFP;Dcx-DsRed* mice by performing multi-photon time-lapse microscopy for 28–36 hr with a fixed 8-min interval. This recording system allowed us to precisely find the three modes of divisions producing the following daughter cells: two progenitors (symmetric divisions) (Figure 3A and Movie S4), a progenitor and an intermediate cell (asymmetric divisions) (Figure 3B and Movie S5), or two intermediate cells (another type of symmetric division) (Figure 3C and Movie S6). These time-lapse recording data revealed that non-terminal symmetric progenitor divisions occurred frequently at P4, which is the early stage of cerebellar neurogenesis, but less frequently at P10, which is the later stage of cerebellar neurogenesis. Among the total cell divisions recorded at P10, 22.09% were non-terminal symmetric divisions (Figure 3D) and 73.58% of the total divisions were terminal symmetric divisions (Figure 3D). The rest (4.33%) were asymmetric divisions that gave rise to a progenitor cell and an intermediate cell from the MATH1-positive progenitor cell. DCX-DSRED-positive cells were not detected right after asymmetric progenitor divisions, suggesting that it is inevitable that MATH1-positive GNPs give rise to cerebellar GNs through intermediate cells during cerebellar neurogenesis and the intermediate cells are a short-time population that exists only at the very early stage of cerebellar development.

Activation of the SHH Pathway Increases the Number of Progenitor Cells by Enhancing Symmetric Cell Divisions

Previous studies have shown that the SHH pathway plays an important role in cerebellar granule neurogenesis (Roussel and Hatten, 2011). PATCHED, a SHH receptor, inhibits the SHH signal pathway by suppressing SMO. Mutation of *Patched* causes an activation of the SHH pathway (Goodrich et al., 1996, 1997). To study whether cell division mode changes mediate the regulation of cerebellar granule neurogenesis governed by SHH signaling, we either performed cell cultures with a SHH signaling activator (C25II) or generated and characterized *Math1-GFP;Dcx-DsRed;Patched*$^{+/-}$ compound mice by crossing the *Math1-GFP;Dcx-DsRed* mice with *Patched*$^{+/-}$ mice (Dahmane and Ruiz i Altaba, 1999).

We first separated the MATH1-positive cells (green), MATH1 and DCX double-positive cells (yellow), and DCX-positive cells (red) from *Math1-GFP;Dcx-DsRed* crossed

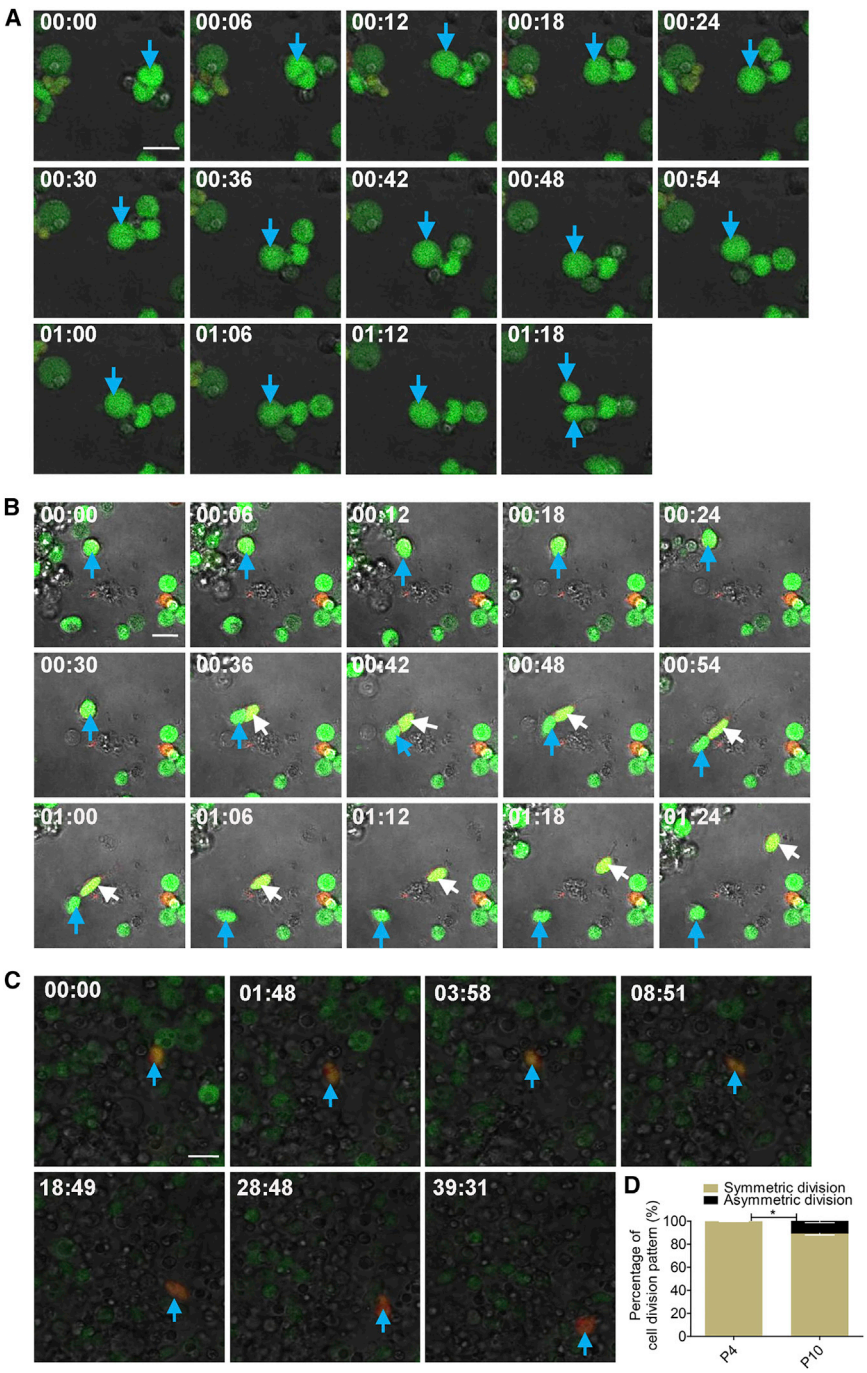

Figure 2. Cerebellar Granule Progenitors Undergo Both Symmetric and Asymmetric Divisions In Vitro

(A) Symmetric division generating two MATH1-GFP daughter progenitors from a MATH1-GFP mother cell was captured by time-lapse recording in cultured GN progenitor cells from *Math1-GFP;Dcx-DsRed* mice (P10). Fourteen selected frames were cropped from a 1.5-hr time-lapse sequence of live image in Movie S2. Images show that a MATH1-GFP cell on the right (blue arrow) undergoes symmetric division.

(B) Images show that a MATH1-GFP mother cell from *Math1-GFP;Dcx-DsRed* mice (P10) undergoes asymmetric division, generating one MATH1-GFP progenitor cell (blue arrow) and one intermediate cell (white arrow) co-expressing MATH1 and DCX. Fifteen selected frames are shown from Movie S3, a 1.5-hr time-lapse sequence.

(C) A MATH1 and DCX co-expressing cell (blue arrow) from *Math1-GFP;Dcx-DsRed* mice (P10) was tracked to show the change gradually into a DCX-expressing cell. Seven selected frames are shown, a 40-hr time-lapse sequence. Scale bars, 20 μm.

(D) Statistical analyses from (A) and (B) show that the ratio of symmetric-to-asymmetric division is 89.23%:10.77% at P10, while all progenitor cells undergo symmetric division at P4 (images not shown).

The data we collected were from 102 dividing cells, which were traced from three independent experiments. Data are shown as mean ± SEM. *$p < 0.05$, referring to the number of symmetric divisions at P4 versus P10.

See also Movies S1 and S2.

mice. We then added recombinant SHH (C25II) to the cultures of MATH1-positive cells (green) from *Math1-GFP;Dcx-DsRed* crossed mice at 0.25 μg/ml. We found that SHH (C25II) promoted the proliferation of GNPs in *Math1-GFP;Dcx-DsRed* crossed mice. The number of MATH1-GFP cells increased 18.89% compared to the control cultures. In control cultures, there were considerable numbers of MATH1 and DCX double-positive (yellow) cells and sole DCX-positive (red) cells (4.75% and 14.11%, respectively; Figure 4). In sharp contrast, no yellow and red cells were seen in the SHH-treated cultures 40 hr after the initial culture (Figure 4).

To study the involvement of cell division modes in the phenotypic changes of cerebellar neurogenesis due to SHH pathway activation in vivo, we performed multi-photon fluorescence microscopy with the freshly

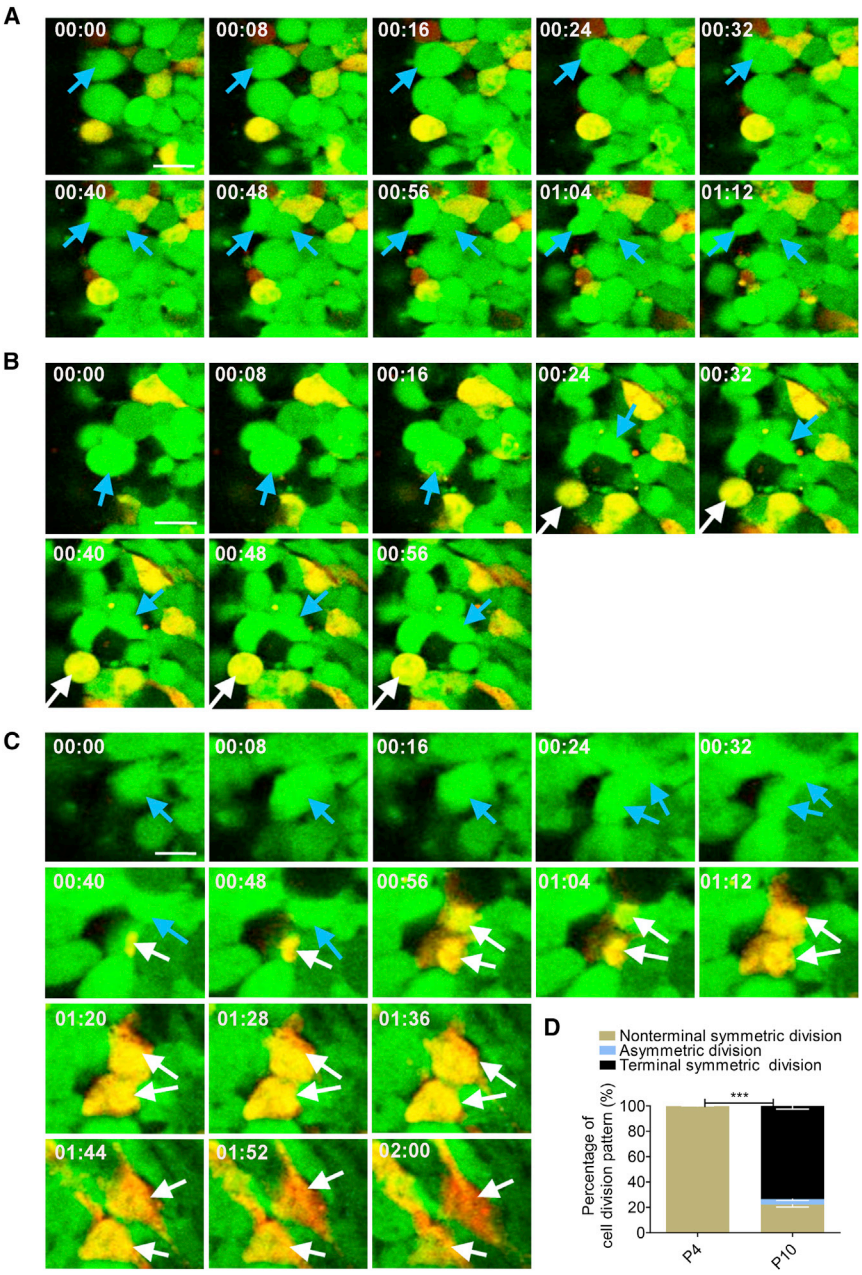

Figure 3. Cerebellar Granule Progenitors Undergo Both Symmetric and Asymmetric Divisions Ex Vivo

(A) Ten selected frames from Movie S4, a 1.5-hr time-lapse sequence of GN progenitor cells. Images show that a MATH1-GFP cell on the left (blue arrow) undergoes symmetric division, generating two MATH1-GFP progenitors (blue arrow).

(B) Eight selected frames from Movie S5, a 1-hr time-lapse sequence. Images show that a MATH1-GFP cell on the left (blue arrow) undergoes asymmetric division, generating one MATH1-GFP progenitor (blue arrow) and one MATH1 and DCX co-expressing cells (white arrow).

(C) Sixteen selected frames from Movie S6, a 2-hr time-lapse sequence. Images show that a MATH1-GFP cell (blue arrow) undergoes symmetric division, generating two MATH1-GFP progenitors (blue arrow). Subsequently, one MATH1-GFP cell on the bottom (blue arrow) slowly turns to yellow (white arrow). Afterward, another MATH1-GFP cell on the top gradually becomes a yellow cell (white arrow). Lastly, both yellow cells change to red, indicating that progenitor cells undergo terminal symmetric division, which is different from the non-terminal symmetric division in (A). Scale bars, 10 μm.

(D) Statistical analysis shows that the ratio of non-terminal symmetric-to-asymmetric-to-terminal symmetric division was 22.09%:4.33%:73.58% at P10, while all progenitor cells undergo symmetric division at P4 (images not shown).

The data we collected were from 77 dividing cells, which were traced from three independent experiments. Data are shown as mean ± SEM. ***$p < 0.001$, referring to the number of non-terminal symmetric divisions at P4 versus P10.

See also Movies S4, S5, and S6.

prepared whole-mount cerebella and then made the three-dimensional (3D) reconstruction of the cerebella from both genotypes (*Math1-GFP;Dcx-DsRed;Patched*$^{+/+}$ and *Math1-GFP;Dcx-DsRed;Patched*$^{+/-}$). As shown in Figure 5A and the statistical analysis in Figure 5B, compared to wild-type mice (*Math1-GFP;Dcx-DsRed;Patched*$^{+/+}$), the number of MATH1 and DCX double-positive cells (intermediate cells, yellow) plus sole DCX double-positive cells (red) decreased by 81.10%, 63.26%, 54.07%, AND 31.63% in *Patched* mutant mice (*Math1-GFP;Dcx-DsRed;Patched*$^{+/-}$) at the P9, P13, P16, and P21 stages, respectively, and the percentage of MATH1-positive cells (progenitor cells) in total cells increased by 25.33%, 23.67%, 29.01%, and 26.35% at P9, P13, P16, and P21, respectively. In addition, in wild-type mice, no intermediate cell was detected at P7 (Figure S2). The in vivo findings are consistent with the in vitro data, suggesting that activation of SHH signaling enhanced the ratio of symmetric cell divisions over the total cell division by reducing the asymmetric divisions so as to delay the differentiation of progenitor cells during cerebellar neurogenesis.

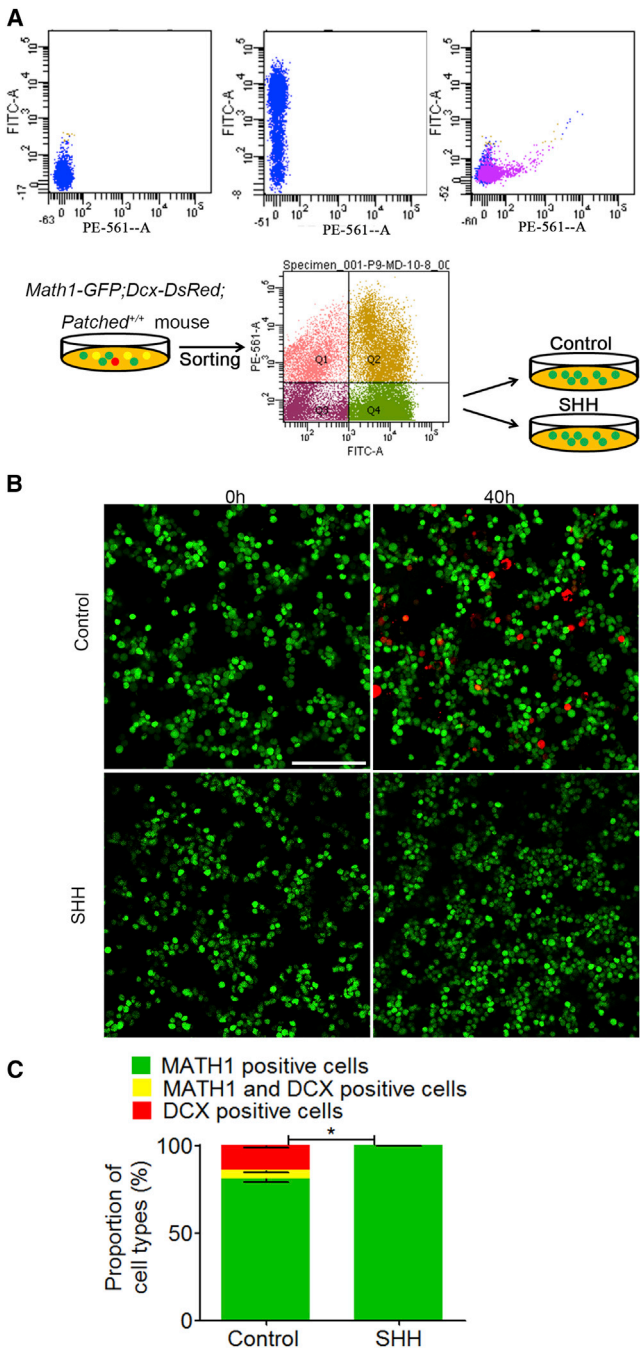

Figure 4. SHH Promotes Proliferation of MATH1-GFP Cells Isolated and Cultured from *Math1-GFP;Dcx-DsRed* Mice In Vitro

SHH (C25II), an activator of SHH pathway, was applied at 0.25 μg/ml to the cultures of MATH1-GFP cells sorted from the cerebella of *Math1-GFP;Dcx-DsRed* mice (P9) by flow cytometry. MATH1-GFP-positive, MATH1 and DCX double-positive, and DCX-positive cells were detected and compared at 0 and 40 hr after drug treatment.

(A) Flow cytometry analysis shows that each population of MATH1-GFP-positive, MATH1 and DCX double-positive, and DCX-positive cells was well separated.

(B and C) There were 4.75% MATH1 and DCX double-positive (yellow) cells and 14.11% sole DCX-positive (red) cells in control cultures. Compared to control cultures, SHH increase the number of MATH1-GFP nearly to 18.86%, and virtually no MATH1 and DCX double-positive cells or DCX-positive cells were found after 40 hr, indicating that SHH prevented the progenitor cells from differentiation.

The data we collected are from four randomly selected visual fields of the culture in each group from three independent experiments. Scale bars, 100 μm. Data are shown as mean ± SEM. *$p < 0.05$, referring to the number of MATH1-positive cells treated with SHH versus vehicle.

Blockade of the SHH Pathway Shifts the Cell Division Modes to Asymmetric Divisions in Cerebellar GNPs in *Math1-GFP;Dcx-DsRed;Patched*$^{+/-}$ Mice Both In Vitro and In Vivo

To investigate whether blockade of the SHH pathway affects the cell division modes of GNPs, we applied cyclopamine (a SHH inhibitor) in cell cultures of GNPs. Cyclopamine (Ma et al., 2013), a naturally occurring steroidal targeting SMO, is regarded as the gold-standard SHH pathway inhibitor (Chen et al., 2002; Drenkhahn et al., 2013). We separated the MATH1-positive cells (green), MATH1 and DCX double-positive cells (yellow), and DCX-positive cells (red) from *Math1-GFP;Dcx-DsRed;Patched*$^{+/-}$ mice at P9. We found that the numbers of MATH1 and DCX double-positive cells and sole DCX-positive cells increased 66.01% and 16.57% (82.58% in total), respectively, in the cyclopamine-treated cultures (10 μM) compared to the vehicle-treated ones 40 hr after the initial culture (Figure 6) to facilitate the differentiation of GNPs in *Math1-GFP;Dcx-DsRed;Patched*$^{+/-}$ mice. Green fluorescent labeling indicates that the cell divisions are symmetric, and red fluorescent labeling or yellow fluorescent labeling show that the cell divisions are asymmetric or terminal symmetric, respectively; these findings implicate that blockade of the SHH pathway by cyclopamine inhibits the non-terminal symmetric progenitor cell divisions and enhances asymmetric progenitor cell divisions and terminal neuronal symmetric divisions.

To confirm the in vitro data that SHH signaling modulates development of the cerebellum by regulating the cell division modes of progenitor cells, we applied cyclopamine, the SHH signaling inhibitor, in *Math1-GFP;Dcx-DsRed;Patched*$^{+/-}$ mice in vivo. We observed a reversing shift from symmetric to asymmetric cell divisions in these mice. As shown in Figure 7, we injected 10 mg/kg of cyclodextrin-associated cyclopamine or cyclodextrin alone as a carrier intraperitoneally in pregnant *Math1-GFP;Dcx-DsRed;Patched*$^{+/-}$ mice from E16 (embryo at day 16) on until P21 (Goodrich et al., 1997; Wetmore et al., 2001) every 3 days. The percentage of progenitor cells (green cells) decreased by 4.93%, 17.58%, 33.67%, and 40.00%

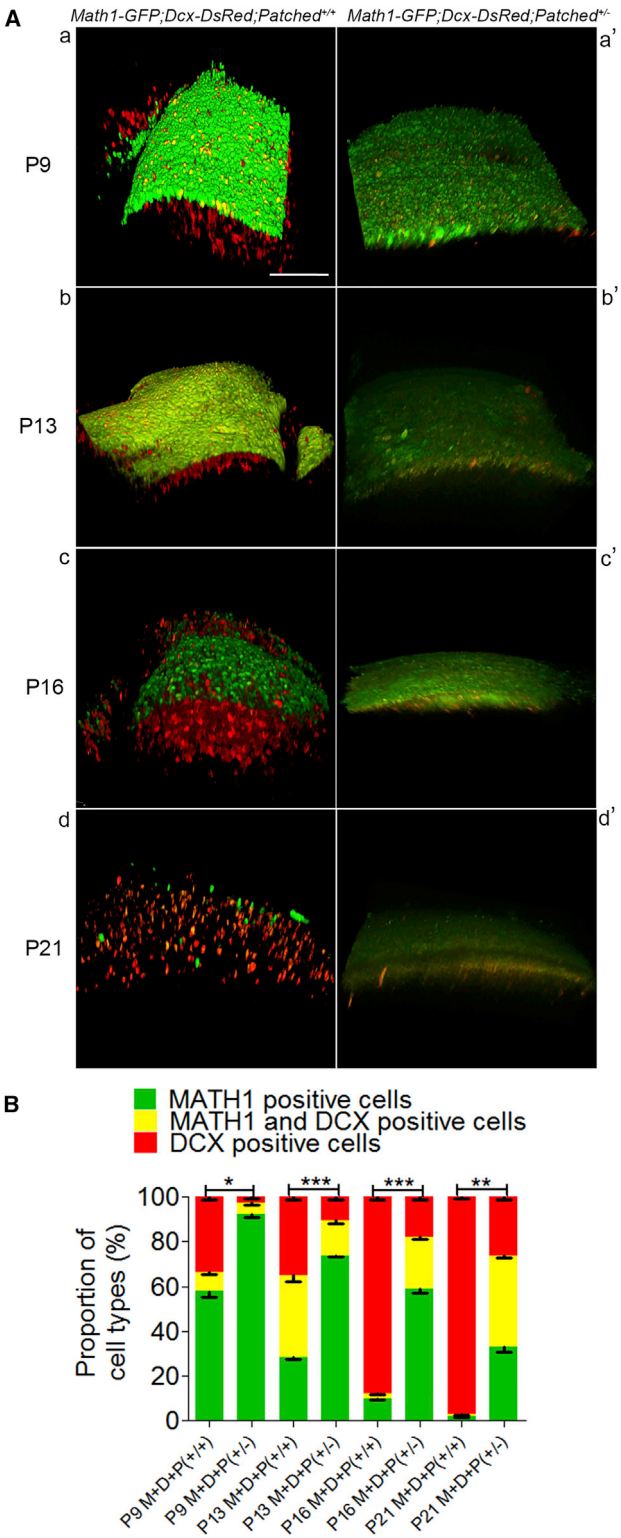

Figure 5. Activation of SHH Pathway Enhances Symmetric Divisions in the Neonatal Cerebellum Ex Vivo

(A) A *Math1-GFP;Dcx-DsRed;Patched*$^{+/-}$ mice strain was developed by crossing *Math1-GFP;Dcx-DsRed* mice and *Patched*$^{+/-}$ mice. *Patched1*, a key factor of SHH pathway, was mutated in *Patched*$^{+/-}$ mice, resulting in activation of hedgehog signaling. 3D images of the cerebella were captured from *Math1-GFP;Dcx-DsRed;Patched*$^{+/+}$ mice (a–d) or *Math1-GFP;Dcx-DsRed;Patched*$^{+/-}$ (a′–d′) mice at P9, P13, P16, and P21, respectively. Scale bars, 100 μm.

(B) Percentages of MATH1-positive cells (green), MATH1 and DCX double-positive cells (yellow), and DCX-positive cells (red) were calculated and compared between the two mouse strains. The results indicate that the percentage of MATH1-positive cells (progenitor cells) over the total cells increased by 25.33%, 23.67%, 29.01%, and 26.35% in *Patched* mutant mice at P9, P13, P16, and P21, respectively, while the number of MATH1 and DCX double-positive cells (intermediate cells, yellow) plus sole DCX double-positive cells (red) decreased significantly in the *Math1-GFP;Dcx-DsRed;Patched*$^{+/-}$ mice. M+D+P$^{(+/+)}$, *Math1-GFP;Dcx-DsRed;Patched*$^{+/+}$ mice; M+D+P$^{(+/-)}$, *Math1-GFP;Dcx-DsRed;Patched*$^{+/-}$ mice.

The data were collected from three animals for *Math1-GFP;Dcx-DsRed;Patched*$^{+/+}$ mice and from five animals for *Math1-GFP;Dcx-DsRed;Patched*$^{+/-}$ mice. Data are shown as mean ± SEM. *p < 0.05, **p < 0.01, ***p < 0.001, referring to the number of MATH1-positive cells in *Math1-GFP;Dcx-DsRed;Patched*$^{+/+}$ versus *Math1-GFP;Dcx-DsRed;Patched*$^{+/-}$ compound mice at P9, P13, P16, and P21.

See also Figure S2.

in *Patched* mutant mice that received cyclopamine at P9, P13, P16, and P21, respectively, compared to mice that received the carrier. Compared with the carrier-treated ones, the total number of red and yellow populations that represent differentiated GNs was significantly increased by 87.50%, 97.72%, 60.74%, and 30.58% at P9, P13, P16, and P21, respectively, in the cyclopamine-treated animals (Figure 7). These data suggest that asymmetric cell divisions are enhanced and the shift to symmetric divisions in the mutant cerebella is reversed by suppression of activated hedgehog signaling during cerebellar granule neurogenesis in the *Patched* mutant mice.

Activation of SHH Signaling Alters the Angles of Spindle Orientation of Dividing GNPs

To explore possible cellular mechanism for the changes of cell division modes regulated by SHH, we performed immunostaining using PH3 as a marker to define the mitosis and spindle orientation angles of dividing GNPs. As shown in Figure S3A, compared to wild-type, *Patched* mutant transgenic mice showed thickened EGL as reported (Goodrich et al., 1997; Wetmore et al., 2000). We found that activation of SHH signaling can change the spindle orientation angles of GNP divisions (Figures S3B–S3D). Spindle orientation was analyzed at P11. In control wild-type cerebella, 20.7% of the spindle orientation were at angles between 0° and 30° relative to the EGL pial surface, 31.0% were at angles between 30° and 60°, and 48.3% were at angles

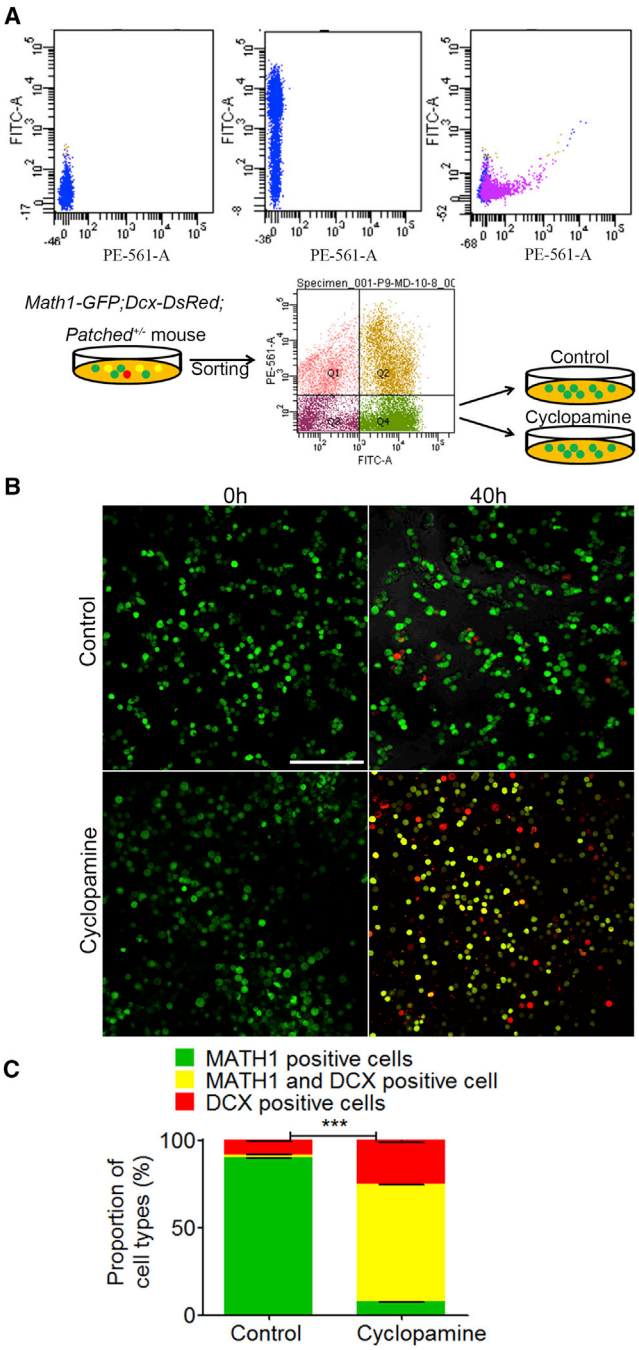

Figure 6. Cyclopamine Largely Reverses Cell Division Mode Shift of GNPs from *Math1-GFP;Dcx-DsRed;Patched*$^{+/-}$ Mice In Vitro

Cyclopamine, an inhibitor of the SHH pathway, was applied at 10 μM to the cultures of MATH1-GFP cells sorted from the cerebella of *Math1-GFP;Dcx-DsRed;Patched*$^{+/-}$ mice by flow cytometry. MATH1-GFP-positive, MATH1 and DCX double-positive, and DCX-positive cells were detected and compared at 0 and 40 hr after drug treatment.

(A) Flow cytometry analysis shows that each population of MATH1-GFP-positive, MATH1 and DCX double-positive, and DCX-positive cells was well separated.

(B and C) Compared to the vehicle, cyclopamine increases the combined number of MATH1/DCX double-positive cells and DCX double-positive cells to 82.58% after 40 hr.

The data we collected are from four randomly selected visual fields of the culture in each group from three independent experiments. Scale bars, 100 μm. Data are shown as mean ± SEM. ***$p < 0.001$, referring to the number of DCX-positive cells and MATH1/DCX double-positive cells treated with cyclopamine versus vehicle.

between 60° and 90° (Figure S3C). In contrast, in *Patched* mutant mouse cerebella, in which SHH signaling is activated, 30.2% of the spindle orientation were at angles between 0° and 30°, 41.3% were at angles between 30° and 60°, and 28.5% were at angles between 60° and 90° (Figure S3C). Statistical analysis indicated that these changes were significant (Figure S3D). Thus, SHH alters cell division modes by inducing spindle orientation changes.

DISCUSSION

Using time-lapse imaging both in vitro and ex vivo and GNP-specific and differentiated GN-specific promoter-driven reporter mice, the present study demonstrated that both symmetric and asymmetric divisions play an important role during cerebellar granule neurogenesis. More importantly, by using a SHH signaling inhibitor, cyclopamine or *Patched* mutant mice, we showed that a balance between asymmetric divisions and symmetric divisions is critical for the regulation of cerebellar granule neurogenesis. While activation of the SHH pathway promotes symmetric divisions, inhibition on the SHH pathway enhances asymmetric divisions of the GNPs. Disregulation of SHH signaling causes a shift from asymmetric division to symmetric division, and such a shift between the two cell division modes can be reversed by administration of the SHH inhibitor cyclopamine. Using PH3, a mitosis marker, we demonstrated that activation of SHH signaling changes cell division modes by altering the angles of spindle orientation of dividing GNPs. Taken together, our work indicates that an appropriate regulation of cell division modes is critical for normal cerebellar granule neurogenesis (Figure S4).

One beauty of our study is that we generated a *Math1-GFP;Dcx-DsRed* double reporter mouse strain to study division modes of GNPs and the cell fate determination process of GNs directly. *Math1* is the murine homolog of the gene *Atoh1* in *Drosophila* (Akazawa et al., 1995; Ben-Arie et al., 1996; Jarman et al., 1993), and it encodes the basic helix-loop-helix transcription factor that is required in the specification of GNPs in the cerebellar EGL (Ben-Arie et al., 1997). In this *Math1-GFP* mouse line, GFP is detected in the GNPs in the developing cerebellum (Lumpkin et al., 2003). However, *Dcx*, a differentiated GN marker,

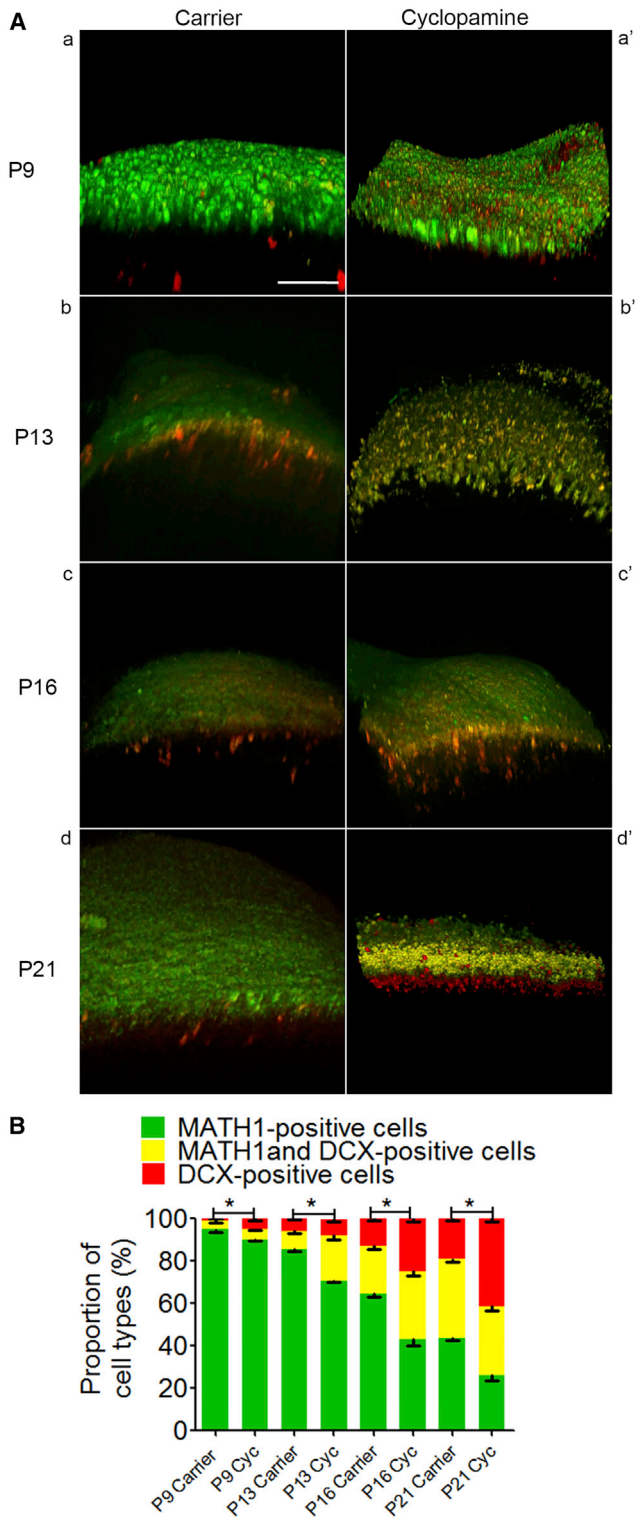

Figure 7. Blockade of SHH Pathway Largely Reverses the Cell Division Mode Shift of GNPs in *Math1-GFP;Dcx-DsRed;Patched*$^{+/-}$ Mice Ex Vivo

(A) Cyclodextrin-associated cyclopamine, an inhibitor of hedgehog signaling, was applied to the transgenic mother mice starting at E16 until P21 every 3 days by intraperitoneal injection at 10 mg/kg (a′–d′). Cyclodextrin alone was used as a carrier (a–d). 3D images of the cerebellum were recorded from *Math1-GFP;Dcx-DsRed;Patched*$^{+/-}$ mice at P9, P13, P16, and P21, respectively. Scale bars, 100 μm.

(B) Percentages of MATH1-positive cells (green), MATH1 and DCX double-positive cells (yellow), and DCX-positive cells (red) were calculated and compared between the carrier and the cyclopamine-treated mice (cyc). The results indicate that the percentages of MATH1-positive cells (progenitor cells) decreased by 4.93%, 17.58%, 33.67%, and 40.00% in *Patched* mutant mice by injection of cyclopamine at P9, P13, P16, and P21, respectively, whereas the number of DCX-positive and MATH1/DCX double-positive cells increased significantly in the cyclopamine-treated mice, indicating that the shift of division modes from asymmetric to symmetric divisions was largely reversed by inhibition of hedgehog signaling during neurogenesis.

The data we collected are from five animals for *Math1-GFP;Dcx-DsRed;Patched*$^{+/-}$ mice and from three animals for cyclopamine-treated *Math1-GFP;Dcx-DsRed;Patched*$^{+/-}$ mice. Data are shown as mean ± SEM. *$p < 0.05$, referring to the number of MATH1-positive cells in the *Patched*$^{+/-}$ compound mutant mice treated with cyclopamine versus carrier at P9, P13, P16, and P21, respectively.

was used as a promoter to drive DSRED expression in DCX-specific cells in *Dcx-DsRed* transgenic mice (Wang et al., 2007). DCX is a microtubule-associated protein that is developmentally regulated in neuronal differentiation and migration (Francis et al., 1999), DCX is also required in cerebellar development (Gleeson et al., 1999). Fluorescence micrographs of cerebellar sections of *Math1-GFP;Dcx-DsRed* mice clearly show that MATH1 and DCX are expressed sequentially by progenitors and differentiated cells. This double reporter mouse line provides us with a powerful and reliable tool to study the neurogenesis of cerebellar development in detail and allows us to keep track of the cerebellar GNPs and their neuronal progenies. In particular, our study suggests that this mouse line appears to be an ideal system for the examination of cell division modes of cerebellar GNPs.

The cells division modes of GNPs in the developing cerebellum are similar to those in the developing cerebrum (Noctor et al., 2004; Taverna et al., 2014) or the CNS of *D. melanogaster* (Bello et al., 2008), but they exhibit differences. In the mammalian cerebrum, neurogenic radial glia progenitors divide asymmetrically to produce a progenitor and a neuron or to produce a progenitor and an intermediate progenitor cell (IPC) that subsequently divides symmetrically to generate two daughter differentiated cells (Noctor et al., 2004). In *D. melanogaster* development, neuroblasts (analogous to murine cerebellar progenitor cells) also undergo two types of asymmetric cell division. One type is that neuroblasts divide asymmetrically to self-renew and generate a ganglion mother cell that subsequently

divides to generate two neurons or two glial cells. The other type is that neuroblasts divide to produce a progenitor and an IPC that subsequently divides to generate a progenitor and a neuron or a glial cell (Bello et al., 2008). The cell division modes of the cerebellar GNPs that we report here resemble type 1 asymmetric cell divisions of neuroblasts during *D. melanogaster* development with a difference. On one hand, the MATH1 and DCX co-expressing cells, which we termed intermediate cells, undergo asymmetric divisions and subsequently generate a differentiated cell. Morphologically, the MATH1-GFP and DCX-DSRED double-positive intermediate cells change gradually from epithelioid cells to polyhedral cells with processes. On the other hand, unlike *D. melanogaster* neuroblasts (Spana and Doe, 1995), progenitor cells in the mammalian cerebellum can also go through terminal symmetric divisions, producing two differentiated cells. In addition, of the 79 MATH1-GFP and DCX-DSRED double-positive intermediate cells examined in time-lapse recording, all turned into red cells gradually and never underwent cell divisions, indicating that they are newborn neurons in the process of differentiation, rather than transient amplifying cells or intermediate neural progenitor or precursor cells identified in the forebrain (Noctor et al., 2004). Our experiments in GNP cell cultures and freshly dissected whole-mount cerebella clearly show that intermediate cells may represent a key step for the generation of the terminally differentiated cerebellar GNs.

A direct and vivid method to follow the progenies of GNPs is to combine both time-lapse imaging and cell-specific promoter-driven report mice. In the present study, we first generated primary cultures of dissociated GNPs from *Math1-GFP;Dcx-DsRed* mice and performed time-lapse recording in the GNP cultures for up to 72 hr after the initial plating. We found that MATH1-positive progenitors can either produce two identical GNPs or generate one GNP and one intermediate cell, which in turn gradually becomes a GN. We then conducted time-lapse 3D imaging acquisition and analysis, which allowed us to explore cerebellar neurogenesis ex vivo in great detail. Consistently, we observed that one MATH1-positive GNP can generate two GNPs by symmetric divisions, one GNP and one intermediate cell, or two intermediate cells. All intermediate cells then gradually turn into GNs. These time-lapse imaging data together vividly show that GNPs can renew themselves by either symmetric or asymmetric division and can produce intermediate cells that in turn become GNs. There is a process of change from intermediate cells to GNs that is marked by downregulation of MATH1 and upregulation of DCX. Therefore, such a time-lapse imaging acquisition technique provides a more dynamic view of the history of the GNPs in cerebellar development than the snapshot view of the developmental status of GNPs by an immunostaining technique.

In this study, we generated *Math1-GFP;Dcx-DsRed;Patched*$^{+/-}$ triple-compound mice to investigate the effect of SHH signaling on cell divisions of progenitors. In this compound mouse line, 14%–20% of mice heterozygous for the *Patched* mutation developed tumors as *Patched* homozygous mice died during embryogenesis (Goodrich et al., 1997; Kim et al., 2003; Oliver et al., 2005; Wetmore et al., 2000). Although it is well known that SHH signaling is associated with the transformation of GNPs in the developing cerebellum, little work has been done on the early stages of the neurogenesis in *Patched* heterozygous mice. The present work indicates that there is a change from asymmetric division to symmetric divisions of the GNPs due to activation of the SHH pathway, which contributes to the development of medulloblastomas (Goodrich et al., 1997). Support for such a shift of the cell division modes triggered by activation of the SHH pathway comes from a recent work in the developing chicken spinal cord (Saade et al., 2013). Given that SHH pathway inhibitors have been shown to be effective in the treatment of medulloblastomas, identification of new molecules, in addition to the inhibitors of the SHH pathway that can restore the asymmetric divisions of the medulloblastomas, may have therapeutic value and are worthy of future study. Furthermore, considering that treatments of CNS diseases and tumorigenesis usually require repair or restoration of the disregulation of a specific process during neurogenesis, our findings of cell division mode modulation of GNPs in normal and *Patched* mutant mice might shed new light on strategies for therapy of cerebellar diseases in the future.

EXPERIMENTAL PROCEDURES

Animals

Math1-GFP transgenic mice (Lumpkin et al., 2003) were provided by Novartis. *Dcx-DsRed* mice (strain name: C57BL/6J-Tg(*Dcx-DsRed*)14Qlu/J, stock number: 009655) and heterozygous *Patched* (*Patched*$^{+/-}$) mice (strain name: STOCK *Ptch1*^{tm1Mps}/J, stock number: 003081) (Goodrich et al., 1997) were obtained from the Jackson Laboratory. *Math1-GFP;Dcx-DsRed* mice were generated by crossing *Math1-GFP* mice with *Dcx-DsRed* mice. *Math1-GFP;Dcx-DsRed;Patched*$^{+/-}$ mice were generated by crossing *Patched* heterozygotes with *Math1-GFP;Dcx-DsRed* mice, confirmed with green and red fluorescence, and genotyped using the following primers for *Patched* mutant mice:

5′-CAC-GGG-TAG-CCA-ACG-CTA-TGT-C-3′ (reverse)
5′-GCC-CTG-AAT-GAA-CTG-CAG-GAC-G-3′ (forward)

All mice were maintained in the Specific-Pathogen-Free Animal Research Centre of Renji Hospital, and all experiments were approved by the Animal Research Ethics Committee of Renji Hospital, School of Medicine, Shanghai Jiao Tong University.

Isolation and Culture of Cerebellar GNPs

Cerebella from P4 or P10 crossed mice were dissected and enzymatically dissociated using papain (Sigma) as described previously (Lee et al., 2005; Wechsler-Reya and Scott, 1999). Briefly, cerebellar tissue was incubated in 10–12 U/ml of activated papain solution plus 32 mg/ml of DNase in DMEM F-12 (Gibco) with rocking for 30 min at room temperature. The tissue was rinsed three times with DMEM F-12 and triturated with a fire-polished glass Pasteur pipette to generate a single-cell suspension. After a single-cell suspension was obtained, cells were plated on coverslips coated with poly-D-lysine (Sigma). Cells were cultured in Neurobasal medium (Invitrogen) supplemented with B-27 (Gibco) (Li et al., 2013a).

Cerebellar Slices

Cerebella were harvested from *Math1-GFP;Dcx-DsRed* mice, embedded in 4% low-melting agarose in liquid Eagle's with Hank's salts and 25 mM HEPES (Gibco), and sectioned at 300 μm using a vibratome (Leica VT1000S). Cerebellar slices were then transferred into 100-ml culture medium containing: 0.5 ml of penicillin/streptomycin solution (stock concentration: 100 U/0.1 mg/ml), 60 mg of Tris (hydroxymethyl) aminomethane (final concentration: 10 mM), 455 μl of a 7.5% $NaHCO_3$ aqueous solution, 25 ml of heat-inactivated horse serum, and 25 ml of 1× Hank's balanced salt solution. Slice cultures were maintained in a humidified incubator at 37°C with a constant 5% CO_2 supply.

Time-Lapse Video Recording

Progenitor cell fate and neuronal differentiation were tracked in vitro using time-lapse video recording. Cells were isolated from *Math1-GFP;Dcx-DsRed* crossed mice, placed into a glass-bottom Petri dish, and maintained in a humidified incubator at 37°C with a constant 5% CO_2 supply. After plating 10 hr, the Petri dish with cells was transferred to a confocal microscope (Nikon) and time-lapse images were acquired with a charge-coupled device (CCD) camera connected to the time-lapse video recorder every 6 min for up to 4 days.

Similarly, progenitor divisions and daughter cell fate determination experiments ex vivo were pursued by 3D reconstruction from multi-photon fluorescence microscope images using time-lapse microscopy (Nikon). Cerebella were harvested from *Math1-GFP;Dcx-DsRed* mice. A Petri dish with freshly dissected whole-mount cerebella was transferred to a multi-photon fluorescence microscope (Nikon), and time-lapse images were acquired with a CCD camera connected to the time-lapse video recorder every 8 min for 28–36 hr (Gogolla et al., 2006). The wavelengths of excitation and emission were 488 and 515 nm, respectively, for GFP and 568 and 590 nm, respectively for DSRED.

SHH and Cyclopamine Treatment

Recombinant mouse SHH (C25II) N terminus (R&D Systems) was applied at a concentration of 0.25 μg/ml for SHH treatment in vitro. Cyclopamine (Selleckchem) was dissolved in ethanol at 10 mM for a stock for cell culture experiments or in PBS containing 45% of 2-hydroxylpropyl-β-cyclodextrin (Sigma) at 1 mg/ml by incubation at 65°C for 1 hr for mouse injections (van den Brink et al., 2001). Aliquots were stored at −20°C until use. For cell culture, the working concentration of cyclopamine was 10 μM. For mouse injections, animals were first injected at E16 and then every other 2 days after birth with 10 mg/kg of cyclopamine or the carrier alone.

Flow Cytometry

Cells dissociated from *Math1-GFP;Dcx-DsRed* or *Math1-GFP;Dcx-DsRed;Patched*$^{+/-}$ mice were digested in papain (Sigma) after 5–10 min and resuspended in single cells. Three independent populations with GFP, DSRED, or GFP/DSRED co-expressing fluorescence were analyzed on a BD FACSAria II cytometer (Becton Dickinson) using standard flow cytometry.

Statistic Analysis

The symmetric and asymmetric division ratio, cell proliferation, and differentiation were analyzed statistically using Student's t test and presented as the mean ± SEM of at least three independent experiments. A two-sided probability value less than 0.05 was considered statistically significant. All plots and data analysis were performed by using Prism GraphPad5.

SUPPLEMENTAL INFORMATION

Supplemental Information includes Supplemental Experimental Procedures, four figures, and six movies and can be found with this article online at http://dx.doi.org/10.1016/j.stemcr.2015.09.019.

AUTHOR CONTRIBUTIONS

W.-Q.G. conceived the experiments. Rong Yang designed and conducted the major experiments and drafted the manuscript. M.W. conducted part of experiments and participated in data collection. X.H. contributed to the experiments of mouse line generation. W.-Q.G. and Ru Yang did the conceptual designs, interpreted the results, and revised and approved the final version of the manuscript.

ACKNOWLEDGMENTS

This research project is supported by funding from the Chinese Ministry of Science and Technology (2012CB966800 and 2013CB945600) to W.-Q.G. and Ru Yang and was supported by the Special Research Foundation of State Key Laboratory of Medical Genomics. W.-Q.G. was also supported by the National Natural Science Foundation of China (81130038 and 81372189), Science and Technology Commission of Shanghai Municipality (Pujiang program), Shanghai Education Committee Key Discipline and Specialty Foundation (J50208), Shanghai Health and Planning Committee Key Discipline and Specialty Foundation, and K.C. Wong Foundation.

Received: March 20, 2015
Revised: September 25, 2015
Accepted: September 25, 2015
Published: October 29, 2015

REFERENCES

Akazawa, C., Ishibashi, M., Shimizu, C., Nakanishi, S., and Kageyama, R. (1995). A mammalian helix-loop-helix factor

structurally related to the product of *Drosophila* proneural gene atonal is a positive transcriptional regulator expressed in the developing nervous system. J. Biol. Chem. *270*, 8730–8738.

Bello, B.C., Izergina, N., Caussinus, E., and Reichert, H. (2008). Amplification of neural stem cell proliferation by intermediate progenitor cells in *Drosophila* brain development. Neural Dev. *3*, 5.

Ben-Arie, N., McCall, A.E., Berkman, S., Eichele, G., Bellen, H.J., and Zoghbi, H.Y. (1996). Evolutionary conservation of sequence and expression of the bHLH protein Atonal suggests a conserved role in neurogenesis. Hum. Mol. Genet. *5*, 1207–1216.

Ben-Arie, N., Bellen, H.J., Armstrong, D.L., McCall, A.E., Gordadze, P.R., Guo, Q., Matzuk, M.M., and Zoghbi, H.Y. (1997). *Math1* is essential for genesis of cerebellar granule neurons. Nature *390*, 169–172.

Bertrand, V., and Hobert, O. (2009). Linking asymmetric cell division to the terminal differentiation program of postmitotic neurons in *C. elegans*. Dev. Cell *16*, 563–575.

Chen, J.K., Taipale, J., Cooper, M.K., and Beachy, P.A. (2002). Inhibition of Hedgehog signaling by direct binding of cyclopamine to Smoothened. Genes Dev. *16*, 2743–2748.

Dahmane, N., and Ruiz i Altaba, A. (1999). Sonic hedgehog regulates the growth and patterning of the cerebellum. Development *126*, 3089–3100.

Drenkhahn, S.K., Jackson, G.A., Slusarz, A., Starkey, N.J., and Lubahn, D.B. (2013). Inhibition of hedgehog/Gli signaling by botanicals: a review of compounds with potential hedgehog pathway inhibitory activities. Curr. Cancer Drug Targets *13*, 580–595.

Francis, F., Koulakoff, A., Boucher, D., Chafey, P., Schaar, B., Vinet, M.C., Friocourt, G., McDonnell, N., Reiner, O., Kahn, A., et al. (1999). Doublecortin is a developmentally regulated, microtubule-associated protein expressed in migrating and differentiating neurons. Neuron *23*, 247–256.

Gao, P., Postiglione, M.P., Krieger, T.G., Hernandez, L., Wang, C., Han, Z., Streicher, C., Papusheva, E., Insolera, R., Chugh, K., et al. (2014). Deterministic progenitor behavior and unitary production of neurons in the neocortex. Cell *159*, 775–788.

Gao, W.Q., and Hatten, M.E. (1993). Neuronal differentiation rescued by implantation of Weaver granule cell precursors into wild-type cerebellar cortex. Science *260*, 367–369.

Gao, W.O., Heintz, N., and Hatten, M.E. (1991). Cerebellar granule cell neurogenesis is regulated by cell-cell interactions in vitro. Neuron *6*, 705–715.

Gleeson, J.G., Lin, P.T., Flanagan, L.A., and Walsh, C.A. (1999). Doublecortin is a microtubule-associated protein and is expressed widely by migrating neurons. Neuron *23*, 257–271.

Gogolla, N., Galimberti, I., DePaola, V., and Caroni, P. (2006). Preparation of organotypic hippocampal slice cultures for long-term live imaging. Nat. Protoc. *1*, 1165–1171.

Goodrich, L.V., Johnson, R.L., Milenkovic, L., McMahon, J.A., and Scott, M.P. (1996). Conservation of the hedgehog/patched signaling pathway from flies to mice: induction of a mouse patched gene by Hedgehog. Genes Dev. *10*, 301–312.

Goodrich, L.V., Milenković, L., Higgins, K.M., and Scott, M.P. (1997). Altered neural cell fates and medulloblastoma in mouse patched mutants. Science *277*, 1109–1113.

Hatten, M.E., and Heintz, N. (1995). Mechanisms of neural patterning and specification in the developing cerebellum. Annu. Rev. Neurosci. *18*, 385–408.

Jarman, A.P., Grau, Y., Jan, L.Y., and Jan, Y.N. (1993). Atonal is a proneural gene that directs chordotonal organ formation in the *Drosophila* peripheral nervous system. Cell *73*, 1307–1321.

Kim, J.Y., Nelson, A.L., Algon, S.A., Graves, O., Sturla, L.M., Goumnerova, L.C., Rowitch, D.H., Segal, R.A., and Pomeroy, S.L. (2003). Medulloblastoma tumorigenesis diverges from cerebellar granule cell differentiation in patched heterozygous mice. Dev. Biol. *263*, 50–66.

Knoblich, J.A. (2008). Mechanisms of asymmetric stem cell division. Cell *132*, 583–597.

Lee, A., Kessler, J.D., Read, T.A., Kaiser, C., Corbeil, D., Huttner, W.B., Johnson, J.E., and Wechsler-Reya, R.J. (2005). Isolation of neural stem cells from the postnatal cerebellum. Nat. Neurosci. *8*, 723–729.

Li, P., Du, F., Yuelling, L.W., Lin, T., Muradimova, R.E., Tricarico, R., Wang, J., Enikolopov, G., Bellacosa, A., Wechsler-Reya, R.J., and Yang, Z.J. (2013a). A population of Nestin-expressing progenitors in the cerebellum exhibits increased tumorigenicity. Nat. Neurosci. *16*, 1737–1744.

Li, X., Erclik, T., Bertet, C., Chen, Z., Voutev, R., Venkatesh, S., Morante, J., Celik, A., and Desplan, C. (2013b). Temporal patterning of *Drosophila* medulla neuroblasts controls neural fates. Nature *498*, 456–462.

Lumpkin, E.A., Collisson, T., Parab, P., Omer-Abdalla, A., Haeberle, H., Chen, P., Doetzlhofer, A., White, P., Groves, A., Segil, N., and Johnson, J.E. (2003). *Math1*-driven GFP expression in the developing nervous system of transgenic mice. Gene Expr. Patterns *3*, 389–395.

Ma, H., Li, H.Q., and Zhang, X. (2013). Cyclopamine, a naturally occurring alkaloid, and its analogues may find wide applications in cancer therapy. Curr. Top. Med. Chem. *13*, 2208–2215.

Machold, R., and Fishell, G. (2005). *Math1* is expressed in temporally discrete pools of cerebellar rhombic-lip neural progenitors. Neuron *48*, 17–24.

Nishiyama, A., Komitova, M., Suzuki, R., and Zhu, X. (2009). Polydendrocytes (NG2 cells): multifunctional cells with lineage plasticity. Nat. Rev. Neurosci. *10*, 9–22.

Noctor, S.C., Martínez-Cerdeño, V., Ivic, L., and Kriegstein, A.R. (2004). Cortical neurons arise in symmetric and asymmetric division zones and migrate through specific phases. Nat. Neurosci. *7*, 136–144.

Oliver, T.G., Read, T.A., Kessler, J.D., Mehmeti, A., Wells, J.F., Huynh, T.T., Lin, S.M., and Wechsler-Reya, R.J. (2005). Loss of patched and disruption of granule cell development in a preneoplastic stage of medulloblastoma. Development *132*, 2425–2439.

Roussel, M.F., and Hatten, M.E. (2011). Cerebellum development and medulloblastoma. Curr. Top. Dev. Biol. *94*, 235–282.

Ryder, E.F., and Cepko, C.L. (1994). Migration patterns of clonally related granule cells and their progenitors in the developing chick cerebellum. Neuron *12*, 1011–1028.

Saade, M., Gutiérrez-Vallejo, I., Le Dréau, G., Rabadán, M.A., Miguez, D.G., Buceta, J., and Martí, E. (2013). Sonic hedgehog signaling switches the mode of division in the developing nervous system. Cell Rep. *4*, 492–503.

Spana, E.P., and Doe, C.Q. (1995). The prospero transcription factor is asymmetrically localized to the cell cortex during neuroblast mitosis in *Drosophila*. Development *121*, 3187–3195.

Taverna, E., Götz, M., and Huttner, W.B. (2014). The cell biology of neurogenesis: toward an understanding of the development and evolution of the neocortex. Annu. Rev. Cell Dev. Biol. *30*, 465–502.

van den Brink, G.R., Hardwick, J.C., Tytgat, G.N., Brink, M.A., Ten Kate, F.J., Van Deventer, S.J., and Peppelenbosch, M.P. (2001). Sonic hedgehog regulates gastric gland morphogenesis in man and mouse. Gastroenterology *121*, 317–328.

Wang, X., Qiu, R., Tsark, W., and Lu, Q. (2007). Rapid promoter analysis in developing mouse brain and genetic labeling of young neurons by doublecortin-*DsRed*-express. J. Neurosci. Res. *85*, 3567–3573.

Wang, X., Tsai, J.W., Imai, J.H., Lian, W.N., Vallee, R.B., and Shi, S.H. (2009). Asymmetric centrosome inheritance maintains neural progenitors in the neocortex. Nature *461*, 947–955.

Wechsler-Reya, R.J., and Scott, M.P. (1999). Control of neuronal precursor proliferation in the cerebellum by Sonic Hedgehog. Neuron *22*, 103–114.

Wetmore, C., Eberhart, D.E., and Curran, T. (2000). The normal patched allele is expressed in medulloblastomas from mice with heterozygous germ-line mutation of patched. Cancer Res. *60*, 2239–2246.

Wetmore, C., Eberhart, D.E., and Curran, T. (2001). Loss of p53 but not ARF accelerates medulloblastoma in mice heterozygous for patched. Cancer Res. *61*, 513–516.

Zhong, W. (2008). Timing cell-fate determination during asymmetric cell divisions. Curr. Opin. Neurobiol. *18*, 472–478.

Zhong, W., and Chia, W. (2008). Neurogenesis and asymmetric cell division. Curr. Opin. Neurobiol. *18*, 4–11.

Zhou, Y., Atkins, J.B., Rompani, S.B., Bancescu, D.L., Petersen, P.H., Tang, H., Zou, K., Stewart, S.B., and Zhong, W. (2007). The mammalian Golgi regulates numb signaling in asymmetric cell division by releasing ACBD3 during mitosis. Cell *129*, 163–178.

Stem Cell Reports, Volume *5*

Supplemental Information

Cell Division Mode Change Mediates the Regulation of Cerebellar Granule Neurogenesis Controlled by the Sonic Hedgehog Signaling

Rong Yang, Minglei Wang, Jia Wang, Xingxu Huang, Ru Yang, and Wei-Qiang Gao

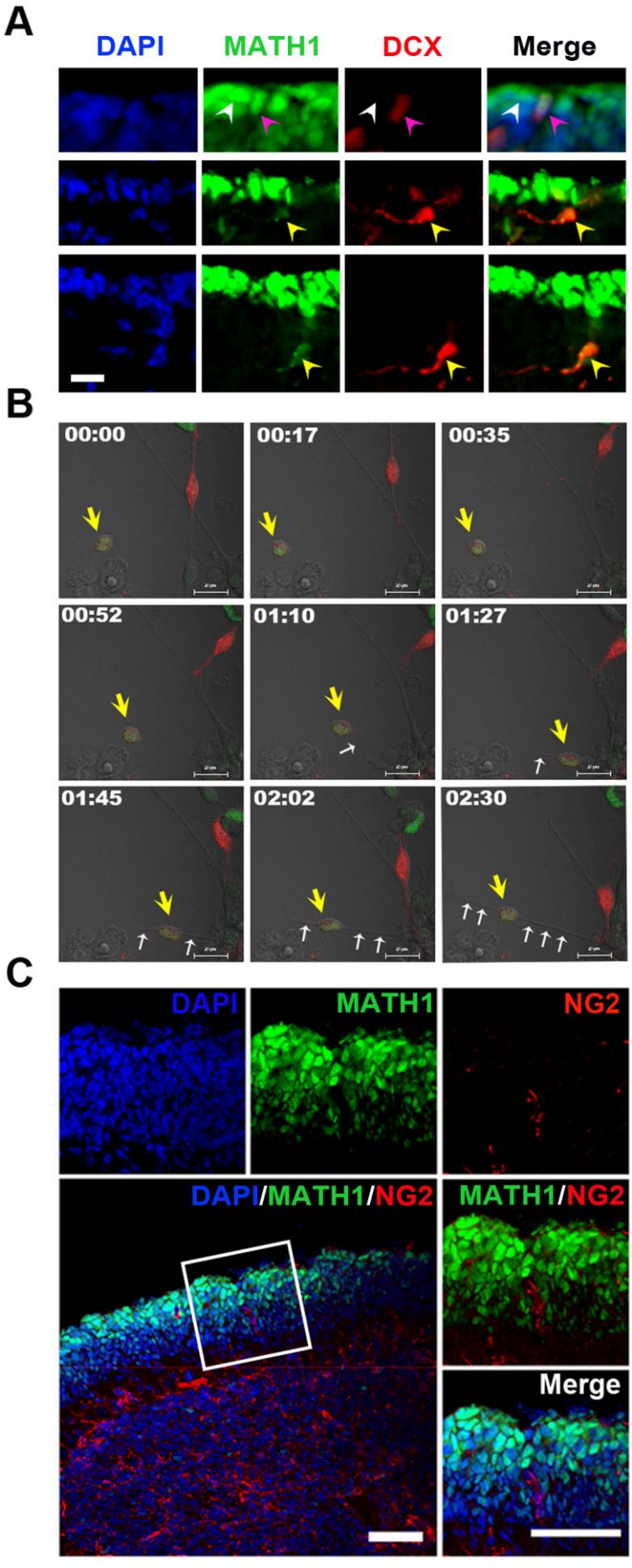
A
DAPI
MATH1
DCX
Merge
B
00:00
00:17
00:35
00:52
01:10
01:27
01:45
02:02
02:30
C
DAPI
MATH1
NG2
DAPI/MATH1/NG2
MATH1/NG2
Merge

Figure S1. Granule neuronal progenitors (GNPs) look like "epitheloid cells" *in vivo*. (A) Confocal images of sagittal sections from the *Math1-GFP; Dcx-DsRed* mouse cerebellum at P11. In the upper panel, white arrowheads indicate MATH1-GFP GNPs and purple arrowheads indicate MATH1-GFP/DCX-DSRED double positive intermediate cells without process. In the medium panel, yellow arrowheads indicate MATH1-GFP/ DCX-DSRED double positive intermediate cells with processes in EGL. In the lower panel, yellow arrowheads indicate MATH1-GFP/ DCX-DSRED double positive intermediate cells with processes in the deeper layer of EGL. Scale bars: 10 μm. (B) Nine selected frames from Movie 1, a 2.5-h time-lapse sequence of MATH1-GFP and DCX-DSRED double positive intermediate cells. The images show that neuronal processes (indicated by small white arrows) extended gradually from yellow intermediate cells (indicated by yellow arrows), which change from epitheloid cells to polyhedral cells. Scale bars: 20 μm. (C) Confocal images of sagittal sections from the *Math1-GFP* mouse cerebellum at P9. NG2 (red) was used to stain polyhedral cells. GNPs were not stained by NG2 antibody. Scale bars: 50 μm. See also Movie 1. Figure S1 related to Results.

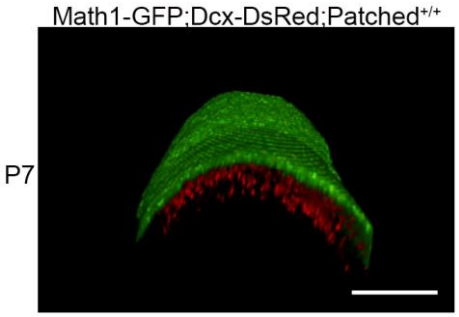

Figure S2. No intermediate cell is detected in wild type mice at P7. By performing multi-photon fluorescence microscopy, we examined the three-dimensional (3D) reconstruction of cerebella in freshly dissected whole mount cerebella from *Math1-GFP; Dcx-DsRed; Patched*$^{+/+}$ mouse strain. We did not detect intermediate cells (yellow) in the *Math1-GFP; Dcx-DsRed; Patched*$^{+/+}$ mouse strain at P7 during cerebellar neurogenesis. Scale bars: 100 μm. Figure S2 related to Figure 5.

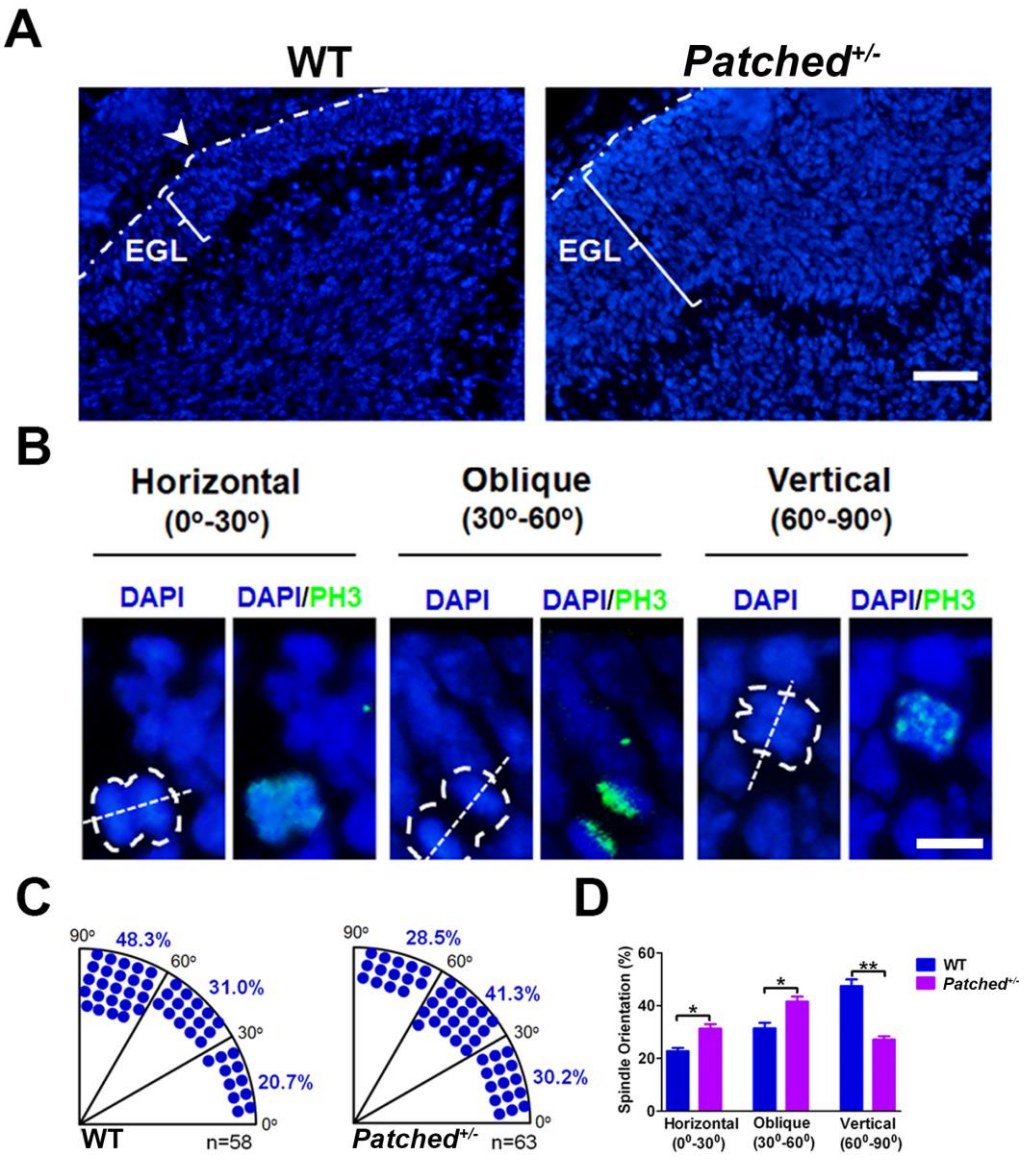

Figure S3. Activation of SHH signaling can alter spindle orientation of GNPs divisions. (A) Activation of SHH signaling enhances the thickness of EGL during cerebellum development as reported. The white arrowhead indicates the EGL pial surface. Scale bars: 50 μm. (B) Examples of three different classes of GNPs divisions, horizontal, oblique or vertical to the pial surface of the cerebellum at P11. PH3 (green) marks mitotic DNA and spindle orientations. DAPI (blue) was used as nuclear counterstain. Scale bars: 5 μm. (C and D) Angle distribution of spindle orientation in GNPs from wild type and *Patched*$^{+/-}$ mouse cerebella (C) and statistic analysis of the angles of spindle orientation (D). The data we collected are from 58 dividing cells in wild type mice and from 63 dividing cells in *Patched*$^{+/-}$ mice, which were from 3 independent experiments. Data are shown as mean ± s.e.m.. *P<0.05, ** P<0.01, referring to the numbers of horizontal, oblique or vertical divisions in wild type vs *Patched* mutant mouse cerebella at P11. Figure S3 related to Results.

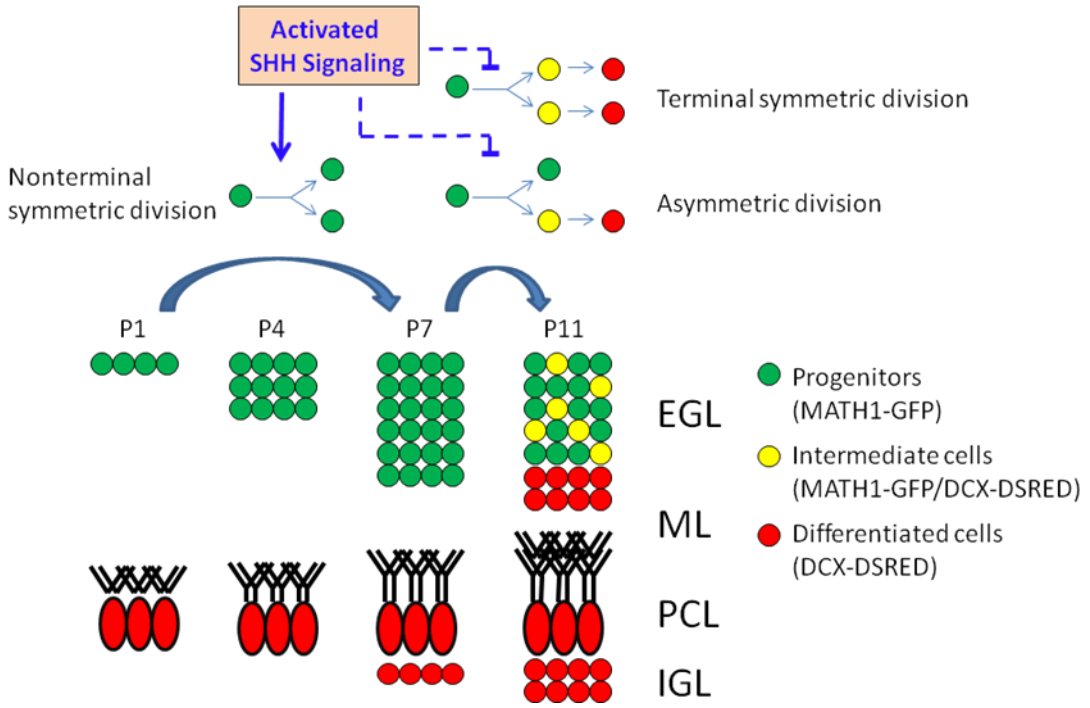

Figure S4. Cell division modes and SHH signaling in cerebellar neurogenesis. A model proposed to indicate that the change of non-terminal symmetric, terminal symmetric and asymmetric cell divisions mediates the regulation of cerebellar granule neurogenesis governed by the sonic hedgehog signaling. Figure S4 related to Discussion.

Movie 1. The morphological change of MATH1-GFP and DCX-DSRED double positive intermediate cells. A 2.5-h time-lapse sequence of live images for MATH1-GFP and DCX-DSRED double positive intermediate cells shows that neuronal processes (indicated by small white arrows) extend gradually from yellow intermediate cells (indicated by yellow arrows), indicating that MATH1-GFP/ DCX-DSRED double positive intermediate cells are morphologically at the stage of changing from epitheloid cells to polyhedral cells. Movie 1 related to Figure S1.

Movie 2. Representative symmetric division of granule neuron progenitor cells *in vitro*. Symmetric division generating two MATH1-GFP daughter progenitors from a MATH1-GFP mother cell was captured by time-lapse recording in cultured granule neuron progenitor cells from *Math1-GFP; Dcx-DsRed* mice (P10). A 1.5-h time-lapse sequence of live image shows that a MATH1-GFP cell on the right (blue arrow) undergoes a symmetrically division. Movie 2 related to Figure 2.

Movie 3. Representative asymmetric division of granule neuron progenitor cells *in vitro*. A 1.5-h time-lapse sequence of live images shows that a MATH1-GFP mother cell from *Math1-GFP; Dcx-DsRed* mice (P10) undergoes an asymmetric division, generating one MATH1-GFP progenitor cell (blue arrow) and one intermediate cell (white arrow) which co-expressing MATH1 and DCX. Movie 3 related to Figure 2.

Movie 4. Representative non-terminal symmetric division of granule neuron progenitor cells *ex vivo*. A 1.5-h time-lapse sequence of live images for granule neuron progenitor cells shows that a MATH1-GFP cell on the left (blue arrow) undergoes symmetric division, generating two MATH1-GFP progenitors (blue arrow). Movie 4 related to Figure 3.

Movie 5. Representative asymmetric division of granule neuron progenitor cells *ex vivo*. A 1-h time-lapse live image recording shows that a MATH1-GFP cell on the left (blue arrow) undergoes an asymmetric division, generating one MATH1-GFP progenitor (blue arrow) and one MATH1 and DCX co-expressing cells (white arrow). Movie 5 related to Figure 3.

Movie 6. Representative terminal symmetric division of granule neuron progenitor cells *ex vivo*. A 2-h time-lapse live image recording shows that a MATH1-GFP cell (blue arrow) undergoes terminal symmetric division, generating two DCX-DSRED differentiated cells (red). Movie 6 related to Figure 3.

Supplemental Experimental Procedures

Histo-immunofluorescence staining

Cerebella were collected from mice and fixed overnight in 4% paraformaldehyde. After incubated sequentially in PBS buffer with 10% and 30% sucrose, the tissue specimens were frozen in embedding medium (O.C.T compound) and sectioned into 10μm thick slices for immunofluorescent staining.

For immunofluorescence staining, tissue specimens were blocked in PBS with 10% donkey serum or 10% goat serum for 1 hour at RT. After blocking, specimens were incubated overnight with rabbit anti-NG2 (Abcam) at 1:500, and mouse anti-PH3 (Cell Signaling Technology) at 1:500. Following 3 times of washes in PBS, specimens were incubated with secondary antibodies conjugated either with Alexafluor 488 or Alexafluor 594 (Jackson Lab) at a 1:600 dilution for 1 hour.

Coverslips were mounted on a slide using a mounting medium containing DAPI. Slides were stored at 4^0C and images were taken within one week. Images were acquired with a Leica confocal microscope and analyzed with LCS confocal software (Leica).